Modelling Enzymatic Reduction of 2-keto-D-glucose by Suspended Aldose Reductase

G. Maria[a,*] and M. D. Ene[a,b]

[a]University Politehnica of Bucharest, Department of Chemical & Biochemical Engineering, Polizu Str. 1, 011061 Bucharest, P.O. 35-107, Romania

[b]Biotehnos Co. s.a., R&D Department, Gorunului Str. 3-5, 075100 Otopeni, Romania

Original scientific paper
Received: February 14, 2013
Accepted: March 26, 2013

Batch experiments have been systematically carried out at 25 °C, pH = 7, over 24-76 h reaction time in order to evaluate the activity of a commercial (recombinant human) aldose reductase (ALR) used to catalyze the reduction of 2-keto-D-glucose (kDG) to fructose using NADPH as cofactor, by employing various enzyme/reactants initial ratios. A kinetic model was proposed by extending the 'core' reaction mechanism proposed in literature for the reduction of several saccharides and keto-derivates (glucose, galactose, xylose, glyceraldehydes) by the human or animal ALR (wild or modified), or by similar aldo-keto reductases (e.g. sorbitol dehydrogenase, xylose reductase) in the presence of NAD(P)H. The reaction pathway assumes a very quick reversible formation of a stable ALR•NADPH complex, from which a small fraction is binding the substrate thus determining a succession of Bi-Bi reversible reactions leading to the final product (fructose). Model parameters have been estimated based on the recorded data sets of four observable key-species, being in concordance with the reported values in literature for similar processes. The results confirm the conformational change of E•$NADP^+$ complex allowing the release of $NADP^+$ as being the rate-limiting step of the overall process. The results also underline the necessity to stabilize the fast deactivating enzyme by immobilization, as well as the requirement of a continuous *in-situ* regeneration of the cofactor.

Key words:
Keto-glucose reduction to fructose, aldose reductase, reaction mechanism, kinetic model

Introduction

Genetically engineered enzymes of modified structure are proved very effective biocatalysts for many biosyntheses of industrial interest, which tend more and more to replace some of the classical fine chemical synthesis processes. Engineered enzymatic reactions, displaying a high selectivity and specificity, are sustainable bioengineering routes to obtain a wide range of biochemical products in food, pharmaceutical, detergent, textile industry, bio-renewable energy industries, or present challenging applications in medicine.[1,2] Biocatalytic processes produce fewer by-products, consume less energy, and generate less environmental pollution, require smaller catalyst concentrations and moderate reaction conditions. However, the crucial aspect in any realistic engineering analysis for process design, operation, control, and optimization relies on the knowledge of an adequate and sufficiently reliable mathematical model. Such a model, preferably based on the process mechanism and developed at various detailing levels (enzyme, reaction, reactor, process, separately identified and linked using specific methodologies), has to ensure interpretable and reliable predictions of the process behaviour under varied operating conditions.[2–4]

In particular, special attention was paid over the decades to aldose reductase (EC 1.1.1.21, aldehyde reductase), being justified by its medical applications: involvement of ALR in the glucose metabolism (glucose conversion to sorbitol, galactose reduction to galactitol), development of diabetic cataract (leading to eye and nerve damage due to sorbitol overproduction),[5] of the myocardial ischemic injury,[6] and other putative physiological processes related to steroid and catecholamine metabolism.[7] As a member of the aldo-keto reductase superfamily,[7] the ALR catalyzes the NADPH-dependent unspecific reduction of a wide variety of carbonyl-containing aliphatic and aromatic compounds to their corresponding alcohols, and especially of aldoses, and corticosteroids (although the enzyme can also utilize the cheaper NADH instead).[8,9] For such reasons, ALR has high potential for industrial applications, e.g. for the production of

*Corresponding author: Tel: +40 744 830308,
E-mail: gmaria99m@hotmail.com

polyols largely used as sweeteners (e.g. sorbitol, mannitol, xylitol, erythritol),[10] for the production of chiral hydroxy-beta-lactams,[11] of arabitol, or of ribitol.[12] ALR can also be used for glucose transformation to fructose, either by glucose reduction to sorbitol followed by its oxidation to fructose (catalyzed by sorbitol dehydrogenase),[13] or by oxidation of glucose to keto-glucose followed by the reduction of the latter to fructose (Cetus process).[14]

ALR is a small monomeric protein, with a molecular mass of 34–43 kDa depending on the enzyme source, present in most of animal cells (liver, kidney, lens, retina, muscles, peripheral nerves, red blood cells, etc.).[15] The commercially purified recombinant ALR, including 315 aminoacid residues, is produced by expressing the human ALR in *E. coli*. Even if presenting multiple forms,[7,16–18] the basic ALR structure consists of a β/α-"barrel" motif made up of eight parallel β strands, the adjacent strands being connected by eight peripheral α-helical segments. The larger active hydrophobic catalytic site is situated in the barrel core, where the cofactor NADPH binds in an extended conformation. The catalytic carbon C4 of the nicotinamide ring of $NADP^+$ is located at the bottom of a deep cleft and having the pyrophosphate straddling the barrel lip.[7,9,19] Aminoacid residues Asp-43, Tyr-48, Lys-77, His-110, Asn-160, and Gln-183, highly conserved in all aldo-ketoreductases, form a tight network of hydrogen bonds linked to the nicotinamide ring (see 3D plots of human ALR given by Blakeley et al.[9]). The tertiary enzyme structure retains considerable flexibility, and many compounds with different chemical structures (inhibitors, activators) can interact with the enzyme in different conformations.

Although ALR is active with both NADPH and NADH coenzymes, the enzyme prefers NADP(H) approximately 2-fold to NAD(H) (in terms of reaction rate), due to better apparent binding of the phosphorylated form of the coenzyme.[20,21] In spite of its higher instability and much higher cost vs. NADH, the NADPH remains the main co-enzyme in ALR catalyzed reactions, with multiple possibilities to be regenerated by means of redox reactions conducted *in-situ* or in separate regenerative systems.[22] Chemical modification of ALR with pyridoxal 5'-phosphate could avoid the oxidation-induced activation, thus increasing its activity.[20]

Optimal ALR activity is reported for temperatures of 25–50 °C and pH = 5.8–10 depending on the substrate used.[23] For instance, an optimum of {50 °C, pH = 6} was found for D-xylose enzymatic reduction with NADH,[20] of {25 °C, pH = 8} for its reduction with NADPH,[24] of {25 °C, pH = 7} for glycolaldehyde reduction,[17] or of {20–37 °C, pH = 6–7} for DL-glyceraldehyde reduction.[8,25]

One potential industrial application is related to the two-step Cetus process for production of high-purity fructose:[14,26] i) D-glucose is firstly converted to kDG in the presence of pyranose 2-oxidase and catalase (to avoid the quick oxidase inactivation),[27,28] at 25–30 °C and pH = 6–7, with very high conversion and selectivity; ii) the kDG is then reduced to D-fructose by NAD(P)H-dependent ALR at 25 °C and pH = 7, the $NAD(P)^+$ being *in-situ* or externally regenerated and re-used.[22,29,30]

When developing an industrial biosynthesis, the engineering aspects related to bioreactor selection, optimal operation and control, are all based on qualitative-quantitative information on the enzyme characteristics (stability, activity, sensitivity to operating conditions and products, deactivation rate, immobilization possibilities), cofactor regeneration, and raw-material characteristics.[31–33] On the one hand, the free-enzyme (semi-)batch operation can be preferred when enzymes exhibit high activity but also a high deactivation rate, and the enzyme is cheap and the product can be easily separated, or its contamination with the enzyme is not important. However, in most cases the use of immobilized enzymes is more advantageous due to easy product separation (with less allergenic enzyme impurities), less enzyme loss, increased enzyme stability (and storage/recycling possibility), enzyme protection against harmful environmental stress, and better control of the process. The enzyme is immobilized on a suitable support (powder, beads, foils, fibres, mesoporous matrices, etc.) made from a large variety of materials (aluminium silicates, ceramics, clay, gels, charcoal, polymers, etc.) tailored to increase enzyme stability with less influence on its activity. Enzyme immobilization methods include: adsorption on solid carriers (through hydrophobic interactions, hydrogen or ionic bonds), entrapment (within the interstitial space of water-insoluble polymers), encapsulation (in gels, lipids, polymers coated with a semi-permeable membrane), covalent-binding (between enzymes and the functionalized support matrix through groups that are not important for catalytic activities of the enzyme), cross-linking (with multifunctional cheap reagents leading to more stable derivatives), and molecular imprinting (by applying specific preparative strategies that place binding or functional groups at defined positions in imprinted sites of the support).[34–40] The advantages and disadvantages of each employed technique are largely presented in the literature. Modern technologies also employ chemical modification of enzymes, or production of modified enzymes by molecular design, prior to their immobilization.[1,38,41] However, enzyme immobilization is costly, and has to be carefully engineered to overcome the significant decrease in activity due to the

matrix-enzyme interactions (changing the enzyme structure), and due to resistance introduced by the diffusion transport through the support. Moreover, when the enzyme deactivation rate is high enough, the use of fixed-/fluidized-bed reactors with immobilized enzymes on solid carriers becomes too costly and inoperable, requiring frequent biocatalyst regeneration/replacement.

One additional engineering aspect to be solved for biocatalytic reactions that use an enzyme cofactor (e.g. NADPH or NADH in the ALR-catalyzed reduction reactions) refers to its continuous regeneration (*in-situ* or externally). Various alternatives can be employed: electron transfer from an electrode via intermediate redox reactions (electrochemical route), parallel enzymatic oxidation reactions (enzymatic routes), (photo)chemical redox reactions, or regeneration using the living cell metabolism (biological route), all being developed in variate continuous systems (membrane, hollow-fibre, packed-beds, or fluidized-beds).[1,22,42–45]

Beside the thermal and chemical stability of the enzyme, one of the key-points in solving the engineering aspects of the process development is related to the knowledge of an adequate process kinetic model based on a formulated reaction pathway. However, modelling complex enzymatic processes involving a significant number of unstable intermediates and steps is a difficult task because the model has to reflect the process complexity under variate operating conditions, starting from a limited number of observed variables recorded with a limited sampling frequency, and often with a low reproducibility due to the enzyme's high sensitivity to the operating conditions. In spite of that, tremendous progress has been made in developing mechanistically-based biochemical process models of various detailing degrees (at biocatalyst, reaction, reactor, and process level),[2] by using comprehensive systematic approaches and mathematical tools. [4,31,46]

In particular, modelling the ALR-catalysed reduction of aldo-keto derivates of saccharides is a steady step due to the involved significant number of unstable intermediates (up to 6)[24] of large molecules linking the substrate, the products, the enzyme and its cofactor (usually NADPH), and difficult to be quantitatively recorded. Various aspects of the ALR catalytic mechanism have been studied, and several models have been proposed, with the identity of the residue donating the proton proving controversial.[9] Recent results suggested that h-ALR may overcome the difficulty of "simultaneously satisfying the requirements of being an effective catalyst and a promiscuous one by using a distal proton donor (Asp-43–Lys-77 pair) acting through the flexible side chain of the final proton donor (Tyr-48)",[9] being thus capable of unspecific accommodating of different substrates. The reaction debuts with the very fast (few seconds)[24] coupling of ALR to NADPH leading to a quite stable complex. However, the substrate presence triggers formation of successive intermediates involving a succession of reversible ordered Bi-Bi reactions.[8,13,17,19] Most of the proposed kinetic models assume that these successive reactions quickly reach their quasi-equilibrium, while the conformation change required for $NADP^+$ release in the last step is rate-limiting for the whole process. To overcome the large number of rate constants of low estimability (leading to estimated lumps),[13,24] some attempts use reduced models assuming a non-competitive substrate /NADPH inhibition,[25] or omit formation of instable enzyme-cofactor-substrate complex (i.e. the Theorell-Chance kinetic mechanism with the enzyme-coenzyme product dissociation being the rate-limiting step for the overall reaction).[19,47,48]

The aim of this work was to study several kinetic aspects of the complex reaction of kDG conversion to fructose using commercial ALR and NADPH. On the one hand, a quantitative analysis of the process kinetics is developed based on systematic batch experiments conducted using suspended ALR (recombined human ALR in *E. coli*) and for various enzyme/reactants initial ratios, in order to check and complete the reaction 'core' mechanism proposed in literature. The estimated model parameters based on the recorded data (key species concentration dynamics) were compared to literature values reported for similar ALR-catalyzed reduction reactions. On the other hand, the modelling analysis reveals some quantitative aspects of practical interest, thus pointing out the rate-limiting step in the direction of substrate reduction, the quasi-stability of the ALR•NADPH complex, the fast deactivation of the enzyme, and the low level of active NADPH in the environment during the reaction. The results clearly indicate the requirement of enzyme stabilization by using a suitable immobilization method, as well as the necessity of continuous *in-situ* regeneration of NADPH cofactor.

Experimental section

Enzymes and reagents

The experiments were conducted in a thermostatically controlled system using commercial grade compounds from Sigma–Aldrich: 2-keto-D-glucose; 2,3,5-triphenyltetrazolium chloride (TTC); 6 N NaOH solution; acetic acid; ethanol; hydrochloric acid; fructose; resorcinol; thiourea; NADPH; 0.01 mol L^{-1} phosphate buffer solution of pH = 7. ALR (EC 1.1.1.21, commercial recombinant enzyme produced by expressing the human ALR in

E. coli; enzyme activity of 0.6 U mg protein^{-1}) was purchased from ATGEN (product number ALR0901). The h-ALR activity was evaluated at 25 °C in 0.1 mol L^{-1} phosphate buffer of pH = 7 in the presence of 10 mmol L^{-1} DL-glyceraldehyde and 0.3 mmol L^{-1} NADPH as substrates (ATGEN test conditions).

The conversion of 2-keto-D-glucose was assessed by applying the same spectrometric procedure described by Maria et al.[27] The detection method is based on a different reduction rate of 2,3,5-triphenyltetrazolium chloride in the presence of various sugars in triphenylformazan. In the present case, the kDG reduces TTC to a red pigment, while fructose presents no effect on the TTC. The analysis uses 0.010 mL sample in a 4 mL test tube, by adding 0.020 mL 1 % aqueous TTC and 0.08 mL 6 N solution of NaOH. After exactly 5 minutes, 3 mL acetic acid:ethanol (1 : 9) is added, and the test tube content is homogenized by inversion. The absorbance of each sample was analysed by spectrophotometry at 480 nm and the unchanged 2-keto-D-glucose content was relatively quantified to a standard curve generated using 2-keto-D-glucose from Sigma.

The decomposition of NADPH can be followed directly by the decrease in absorbance at 340nm (ε_{340} = 6.2 ± 0.3 ·10^3 L mol^{-1} cm^{-1}).[21] Enzymatic activity was confirmed by measuring the amount of enzyme catalyzing the oxidation of 1 μmol L^{-1} NADPH/min. at 25 °C.

Determination of fructose concentration in samples was based on the property of carbohydrates to form furfural in the acid environment, which subsequently reacts with resorcinol to form a red compound. The reaction mixture contained: 80 μL of sample, 40μL of resorcinol reagent (1g resorcinol and 0.25g thiourea dissolved in 100 mL glacial acetic acid), and 0.280 μL of diluted hydrochloric acid (five parts concentrated HCl mixed with one part distilled water). The reaction mixture is heated in a water bath at 80 °C for exactly 10 minutes. The tubes are then cooled by immersing them in tap water for 5 minutes, and absorbance is read at λ = 520 nm within 30 minutes.[49] The fructose content is relatively quantified from a standard curve generated using fructose from Sigma.

Batch experiments of kDG reduction to fructose

Free enzyme experiments were carried out in a small reaction vessel (precision Hellma cells made of Quartz SUPRASIL, of 10 mm thickness), filled with 1.8–2.5 mL reaction liquid, and equipped with an on-line temperature recording system. The sealed milli-reactor (to prevent solvent vaporization) was placed in a UV/VIS spectrophotometer Lambda 25 with a thermostatic mixing system and a PTP-6 temperature-control unit of the following performances: 0–100 °C temperature range, of 0.1 °C readout resolution and ±0.01 °C readout stability, heating/cooling temperature programming rate of 10 °C min^{-1}, 1800 rpm stirrer speed. The reaction was conducted at 25 °C and pH = 7 in a 10 mmol L^{-1} phosphate buffer, with various initial conditions covering the range of [kDG] = 15–35 mmol L^{-1}, [NADPH] = 6–35 mmol L^{-1}, and [ALR] = 0.0026–0.0060 U mL^{-1}. The shaking system (a magnetic stirrer in the cuvette) ensured satisfactory homogenization of the bioreactor content, while the phosphate buffer preserved quasi-constant pH. A slight increase in pH to 7.4 was recorded at the end of the batch due to the environmental H^+ consumption by the main reaction (Table 1). However, the minor pH increase is assumed to present a negligible effect on the enzyme activity as long as the optimum range for the human-type ALR covers the interval pH = 7–8.[23,24]

Even if the NADPH concentration declined sharply at the beginning of the reaction, the progress of the kDG reduction was continuously monitored over large batch times (up to 4600 minutes) to confirm the reversible formation of the ALR•NADPH complex maintaining a low level of NADPH in the reactor, and characterize enzyme deactivation. Small samples taken during the reaction were analysed separately to determine the concentration of kDG (10 μL samples), fructose (80 μL samples) and the ALR residual activity (10 μL samples). Aliquoted samples in vials were immediately stored at –70 °C for future analysis. Enzyme assays and sample analyses were performed in duplicate, leading to an approximate estimate of the noise level for every recorded species, that is the standard deviations of $\sigma_{kDG} = \sigma_P = \sigma_{NADPH}$ = 1.5 mmol L^{-1}, and σ_{ALR} = 10^{-4} U mL^{-1}.

Experiments at low initial concentrations of substrate and NADPH are not interesting from the engineering point of view due to the obtained low conversions and reactor productivity. The recorded dynamic evolution of the main species concentrations, displayed in Figs. 1–4, was further used to estimate the rate constants of the kinetic model.

Modelling the enzymatic process kinetics

Reaction pathway

Several studies from literature indicate that the 'core' mechanism of ALR and NADPH action on aldo-keto derivates involves a succession of several rapid reversible Bi-Bi reactions.[8,13,17,19] Since the equilibrium is reached quickly, quasi-stationarity could be assumed of the transitory complexes

Table 1 – *Kinetics and batch reactor model proposed for keto-D-glucose enzymatic reduction using NADPH and suspended aldose reductase (commercial recombinant ALR obtained by expressing human 1-316aa plasmids in E. coli; enzyme source: ATGEN, Cat. no. ALR-0901). Notations: E = aldose reductase; A = NADPH; A^+ = $NADP^+$; S = kDG (substrate); P = fructose (product)*

Overall reactions:

$$C_6H_{10}O_6\ (S) + NADPH\ (A) + H^+ \xrightarrow[(phosphate\ \ buffer)]{ALR\,(E),\ r_P} C_6H_{12}O_6\ (P) + NADP^+(A^+)$$

$$y\,NADPH + ALR \underset{k_{-d}}{\overset{k_d}{\rightleftharpoons}} (ALR \bullet NADPH_y)$$

$$ALR\ (E) \xrightarrow{r_i} \text{inactive ALR (Ein)}$$

Rate expressions (see scheme of Fig. 5):

$$r_P = \frac{k_p[E_t][S]\left(\frac{[A]}{K_R K_A} - \frac{1}{K_{eq}K_{AP}}\frac{[A^+][P]}{[S]}\right)}{1 + \frac{[A]}{K_A} + \frac{[A][S]}{K_R K_A} + \frac{[A^+]}{K_{AP}}}\text{, (successive Bi-Bi mechanism)}$$

$$r_d = k_d[A][E]\ ;\ r_{-d} = k_{-d}[E^*A]\ ;\ r_i = k_i[E]$$

$$K_A = \frac{[E][A]}{[EA]} = \frac{k_{-a}}{k_a}\ ;\ K_R = \frac{[EA][S]}{[EAS]} = \frac{k_{-r}}{k_r}\ ;\ K_{eq} = \frac{[EA^+][P]}{[EAS]} = \frac{k_p}{k_{-p}}\ ;$$

$$K_{AP} = \frac{[E][A^+]}{[EA^+]} = \frac{k_{ap}}{k_{-ap}}$$

Mass balances in the batch operation mode:

$$-\frac{dS}{dt} = \frac{dP}{dt} = \frac{dA^+}{dt} = r_P$$

$$\frac{dA}{dt} = -r_P - y\,r_d + y\,r_{-d}$$

$$\frac{dE}{dt} = -r_d + r_{-d} - r_i$$

$$\frac{d(E^*A)}{dt} = r_d - r_{-d}$$

Operating parameters:

liquid volume = 1.8–2.5 mL
10 mmol L^{-1} phosphate buffer
pH = 7
25 °C
[kDG] = 0–35 mmol L^{-1}
[NADPH] = 0–35 mmol L^{-1}
initial [ALR] = 0.0026–0.0060 U mL^{-1}

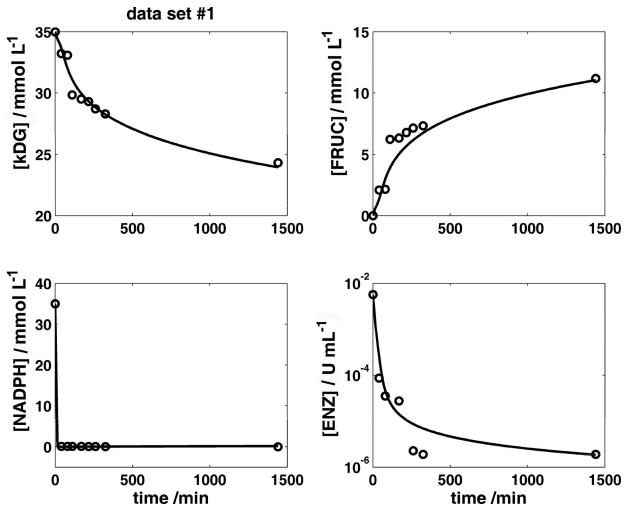

Fig. 1 – *Dynamics of the observable species concentration for keto-D-glucose enzymatic reduction using NADPH and suspended ALR. Initial conditions: 35 mmol L^{-1} kDG, 35 mmol L^{-1} NADPH, 0.0057 U mL^{-1} ALR, 10 mmol L^{-1} phosphate buffer, pH = 7; 25 °C. Model predictions are represented by full line, and experimental values by 'circles'.*

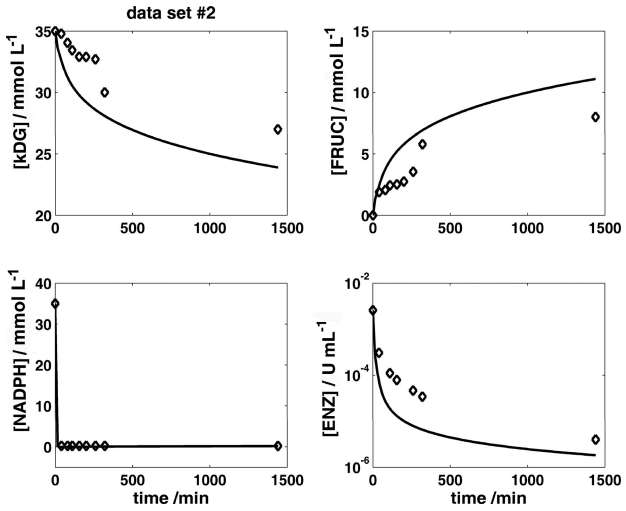

Fig. 2 – *Dynamics of the observable species concentration for keto-D-glucose enzymatic reduction using NADPH and suspended ALR. Initial conditions: 35 mmol L^{-1} kDG, 35 mmol L^{-1} NADPH, 0.00257 U mL^{-1} ALR, 10 mmol L^{-1} phosphate buffer, pH = 7; 25 °C. Model predictions are represented by full continuous line, and experimental values by 'diamonds'.*

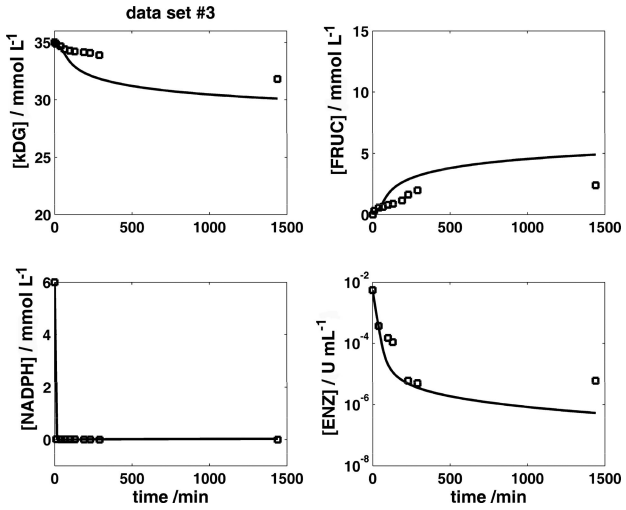

Fig. 3 – *Dynamics of the observable species concentration for keto-D-glucose enzymatic reduction using NADPH and suspended ALR. Initial conditions: 35 mmol L^{-1} kDG, 6 mmol L^{-1} NADPH, 0.0055 U mL^{-1} ALR, 10 mM phosphate buffer, pH = 7; 25 °C. Model predictions are represented by full line, and experimental values by 'squares'.*

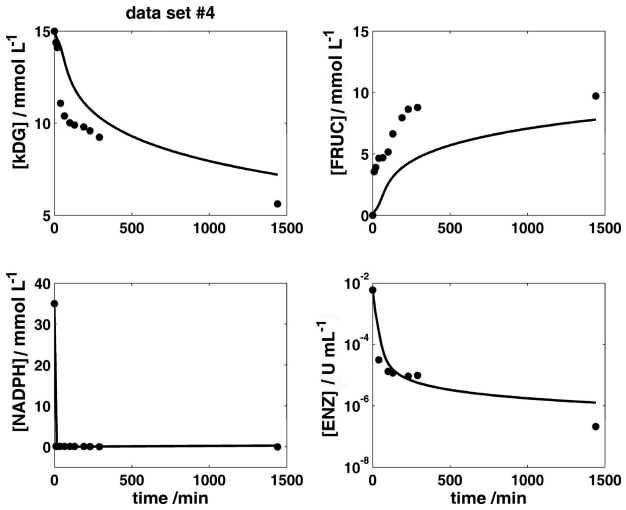

Fig. 4 – *Dynamics of the observable species concentration for keto-D-glucose enzymatic reduction using NADPH and suspended ALR. Initial conditions: 15 mmol L^{-1} kDG, 35 mmol L^{-1} NADPH, 0.006 U mL^{-1} ALR, 10 mmol L^{-1} phosphate buffer, pH = 7; 25 °C. Model predictions are presented by full line, and experimental values by 'stars.*

formed between ALR, NADPH and substrate. Simplified expressions of the overall reaction rate can be derived by including the equilibrium constants of the intermediate steps.[50] Thus, the main reaction pathway proposed for the studied h-ALR catalyzed reduction of kDG with NADPH, is presented in Fig. 5. The main intermediate steps and deactivation side-reactions are the following (with notations E = ALR; A = NADPH; A^+ = $NADP^+$; S = kDG; P = fructose; Ein = inactive form of enzyme):

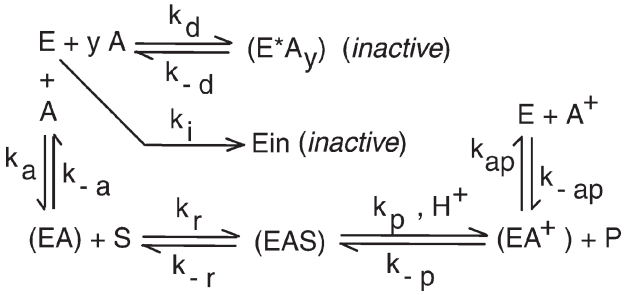

Fig. 5 – *The reaction pathway proposed for keto-D-glucose enzymatic reduction using NADPH and suspended ALR. Notations: E = aldose reductase (ALR); A = NADPH; S = kDG (substrate); P = fructose (product); Ein, (E^*A_y) = inactive forms of the enzyme.*

i) The first very rapid reaction is the A binding to E, in large amounts, to form a quasi-stable complex (E^*A_y), which is inactive for substrate binding, probably due to the transient unfavourable configuration of sites. As experimentally proved by Grimshaw et al.[24] this is a very fast binding reaction (of high k_d much larger than k_{-d} in Table 2), taking place over a few seconds, confirmed by our experimental observations. Most of the reported models in the literature do not consider the formation of this catalytically inactive complex, even if "inactive" forms of ALR have been identified by several authors.[24] This, apparently parallel, reaction is suggested by the experimental evidence in Figs. 1–4, revealing a continuous reaction progress in terms of consumed kDG and formed fructose in spite of the initial, very sharp decrease in [NADPH] from 6–35 mmol L^{-1} to low but quasi-constant levels of 0.1–0.3 mmol L^{-1}. Otherwise, a monotonous [NADPH] trajectory should be expected, similar to the exponential-like [kDG] curve. This experimental evidence suggests that the kDG reduction does not stop due to the NADPH sharp initial decrease, but only slows down, while small amounts of catalytically active (EA) complex are continuously formed triggered by the presence of the substrate.

ii) In parallel, a small fraction of enzyme is rapidly binding to NADPH by forming an active complex (EA) suitable for further coupling the substrate. The reaction can be considered at quasi-equilibrium (of $K_A = k_{-a} / k_a$ constant in Table 2). As remarked by Petrash et al.[19] this enzyme activation "induces a conformational change of enzyme E•A ↔ E'•A that involves hinge-like movement of a surface loop so as to cover a portion of the coenzyme in a fashion similar to a safety belt." The enzyme isomerization is not very rapid, having an average equilibrium constant of O(10^{-1}) (Table 2).[8] As further revealed by the identified model constants, only a small fraction of the enzyme follows this route comparatively to the formation of the inactive (E^*A_y) complex.

Table 2 – *Identified kinetic parameters, significance tests, and literature data for keto-D-glucose enzymatic reduction using NADPH and suspended aldose reductase (kinetic parameters for 25 °C, pH = 7; commercial recombinant ALR from ATGEN, Cat. no. ALR-0901). The t-tests computed with minimum relative noise of* $\tilde{\sigma} = 0.024$ *(see Appendix of Treitz et al.[51] for details)*

Parameter	Estimate (± 95 % CI)[(a)]	*t*-test(a)	Ordered $\lambda_j / \tilde{\sigma}^2$ [(b)]	Reported value
k_p, mM min^{-1} (U/mL)$^{-1}$	$(3.90 \pm 1.20) \cdot 10^6$ (289–1560 min^{-1})	6.3 (√)	1	11–36 (min^{-1}) (substrate of glycolaldehyde,[17] or glyceraldehydes[8]; animal ALR) 9300 min^{-1} (for xylose reductase)[16]
K_A, mmol L^{-1}	50.58 ± 23.85	4.1 (√)	1	10^{-4} – 2740 (various substrates and ALR sources) [23,24,52]
K_R, mmol L^{-1}	1.15 ± 0.21	10.9 (√)	1	0.2–150 (various substrates)[25] 1.06 (xylose substrate; human ALR)[24]
K_{eq}, mmol L^{-1}	1637 ± 417	7.7 (√)	1.6	446–528 (xylose reductase)[16] 200 (xylose substrate; human ALR)[24]
K_{AP}, mmol L^{-1}	0.99 ± 0.40	4.8 (√)	4.8	$1.9 \cdot 10^{-3}$ – $8.3 \cdot 10^{-3}$ (glyceraldehydes)[8] $3 \cdot 10^{-3}$ (xylose substrate; human ALR)[24]
k_d, mM^{-1} min^{-1}	$(2.66 \pm 0.14) \cdot 10^6$	37.7 (√)	9.7	$7.2 \cdot 10^6$ (human ALR)[24]
k_{-d}, min^{-1}	672 ± 35	37.7 (√)	$1.6 \cdot 10^5$	10^4 (human ALR)[24]
y, mM (U/mL)$^{-1}$	$(1.78 \pm 0.01) \cdot 10^4$	2219 (√)	$1.1 \cdot 10^9$	–
k_i, min^{-1}	$(7.01 \pm 0.01) \cdot 10^{-2}$	8162 (√)	$3.5 \cdot 10^{12}$	–
s_y [(c)], (-)	1.04			remark:[(d)] adequacy χ^2 – test passed

(a) a parameter is significant for *t*-test > *t(Nm-p;0.975)* = 1.98 (symbol "√" for passed test), where N = total number of experimental points (39) over four data sets; m = number of observed variables (4); p = number of model parameters (9); 95 % CI = the 95 % confidence interval of the estimate.[3]

(b) ridge selection test of Maria and Rippin[53] is passed when $\lambda_j / \tilde{\sigma}^2 > 1$.[3,51] Values of $\lambda_j / \tilde{\sigma}^2 \approx 1$ correspond to highly intercorrelated parameters, which are difficult to estimate separately (λ_j = eigenvalues of the inverse of the modified parameter covariance matrix).

(c) relative standard error deviation of the model (related to the noise error) was computed with Eq. (1) formula.

(d) model is adequate, the following test being passed: $\chi^2 = 45.6 < \chi^2(Nm\text{-}p;\ 95\ \%) = 176.3$ (√).[3]

iii) The presence of the substrate triggers the formation of an instable complex (EAS) which quickly ($K_{eq} = k_p / k_{-p} >> K_R = k_{-r} / k_r$) leads to fructose-product formation "by transfer of the *pro*-R hydride of NADPH to the *re*-face of the substrate carbonyl carbon".[19] The compulsory-order mechanism involving the formation of the ternary complex was experimentally proved by Ryle and Tipton[21] in the case of pyridine-3-aldehyde reduction, although the complementary iso-Theorell-Chance mechanism cannot be totally excluded [in which the enzyme-substrate complex is oxidized by the electron acceptor so rapidly that the ternary complex (EAS) becomes kinetically insignificant].

iv) After the product release, a second conformation change is required (E'•A$^+$ ↔ E•A$^+$, not explicitly included in the model) in order to release the oxidized coenzyme NADP$^+$. Various kinetic studies proved that this conformation change required for NADP$^+$ release represents the rate-limiting step of the whole process in the direction of substrate reduction, the equilibrium constant $K_{AP} = k_{ap} / k_{-ap}$ being one-two orders of magnitude smaller than all other equilibrium constants from the successive reaction scheme (Table 2).

v) Experimental observations in Figs. 1–4 reveal a quite fast enzyme deactivation, in parallel to other reactions. Even if the complex (E*A$_y$) slow dismemberment partially compensates the active enzyme loss (see enzyme mass balance in Table 1), the inactivation process leads to maintaining a low enzyme level during most of the reaction.

Globally, the overall reduction reaction displayed in Table 1 is accompanied by a side-reversible binding of ALR to the co-enzyme NADPH to form an inactive complex, and by the enzyme deactivation reaction. The present study will check the validity of the successive reversible Bi-Bi reaction scheme in the case of kDG substrate, the characteristics of the side-reactions, the significance of the estimated rate constants, and will use the model predictions to derive practical conclusions of interest for further improvement of the process.

Rate constant identification and results discussion

Based on the proposed reaction pathway in Fig. 4, a hyperbolic expression of the overall reaction rate was derived (Table 1), by assuming rapid equi-

libriums for all elementary steps of the main path, and by eliminating the unobservable intermediate species from the rate equation (see e.g. Segel[50] for details on such a general rule for writing equations for rapid equilibrium systems). The species mass balance also includes the side reactions of reversible enzyme binding to NADPH (of k_d and k_{-d} rate constants), and of enzyme irreversible deactivation. In order not to complicate the kinetic model, a first-order ALR inactivation model was adopted (of k_i deactivation constant).

An ideal batch reactor model was adopted (isothermal, perfectly mixed), in order to simulate the batch experiments, by including the mass balance equations of Table 1. The rate constants were fitted by adjusting the model predictions to match the experimental concentration-time profiles of kDG, fructose, NADPH, and active ALR. The used data sets cover four batch tests by using variate initial conditions in the ratios of [kDG] / [NADPH] / [ALR] = 35 / 35 / 0.0057, 35 / 35 / 0.00257, 35 / 6 / 0.0055, and 15 / 35 / 0.006 (mmol L^{-1}/ mmol L^{-1}/ U mL^{-1}) respectively. A weighted least square criterion was used as statistical estimator of the rate constant vector $\boldsymbol{k}$, by minimizing the relative error variance of the model, that is:[3]

$$\hat{\boldsymbol{k}} = \arg\,\mathrm{Min}\,(s_y^2);$$
$$s_y^2 = \Big(\sum_{j=1}^{m} \left\| \boldsymbol{c}_\mathrm{j} - \hat{\boldsymbol{c}}_\mathrm{j} \right\|_2^2 / \sigma_\mathrm{j}^2\Big) \,/\, \big(N\ \mathrm{m} - p\big), \qquad (1)$$
$$j = \mathrm{kDG, NADPH, fructose, ALR}$$

where: N = the number of experimental points (i.e. 39 reaction times); m = the number of observed variables (4 here); p = the number of model parameters (9 here), '^' = estimated values. The adaptive random optimization algorithm MMA/MMAMI of Maria,[54] implemented in Matlab™, was used as an effective solver. The multimodal search was started from an initial guess of the kinetic parameters randomly generated within the reported variation domain of Table 2 (last column) (except the k_i deactivation constant, which was approximated from the [ALR] experimental plots).

The estimated model parameters for 25 °C are presented in Table 2 together with the associated 95 % confidence interval, and statistical *t*-test of estimate quality. Model predictions displayed in Figs. 1–4 for all data sets (solid lines) are in good agreement with the experimental data (points). The model is globally adequate, while the average relative error of the model s_y = 1.04 is acceptable, being comparable to the experimental minimum relative noise. The analysis of the estimated rate constants (Table 1) and model predictions (Figs. 1–4) leads to several conclusions:

i) in spite of slight overparameterization (i.e. 9 parameters vs. 4 observed variables recorded over 39 runs), the proposed kinetic model is robust and offers adequate predictions irrespective of the chosen initial concentrations of species over the investigated operating domain of [kDG] = 0–35 mmol L^{-1}, [NADPH] = 0–35 mmol L^{-1}, initial [ALR] = 0.0026–0.0060 U mL^{-1}. Such a conclusion could support the adoption of the above-presented 'core' mechanism from literature derived for similar reduction processes, including h-ALR[24] or animal-ALR[17] catalysed reactions.

ii) the statistical tests were roughly passed, i.e. an acceptable model global adequacy (χ^2 test was passed, displaying a smaller value than the theoretical 95 % χ^2-quantile; see Table 2-footnote d), and fairly significant rate constants (i.e. *t*-tests higher than the relevant quantile value of Table 2-footnote a, and most of $\lambda_j / \tilde{\sigma}^2$ test values higher than 1, see Table 2-footnote b). The 95 % confidence intervals of the estimated constants are satisfactorily small, the larger ones corresponding to estimated parameters presenting smaller *t*-tests (K_A, K_{AP}, and k_p). Besides, equal *t*-tests of k_d and k_{-d} constants indicate their high inter-correlation, leading to the impossibility of their separate estimation without additional information. According to the more sensitive $\lambda_j / \tilde{\sigma}^2$ significance test of Maria and Rippin[53], there are three constants of low estimability, corresponding to K_A, K_{AP}, and one of the k_d and k_{-d} constants. Such low estimability for some rate constants of the hyperbolic rate expression models is a common subject in literature when structured information on intermediate dynamics is lacking, some parameters presenting inter-correlation coefficients higher than 0.95–0.99. Consequently, their separate estimation with precision is not possible as long as no experimental measurements concerning the dynamics of instable intermediate species (EA), (EAS), (EA^+) are available.

iii) most of the estimated rate constants present close values or fall within the range of variation of the corresponding rate constants reported in the literature for similar enzymatic reduction processes, even if various sources of ALR (including h-ALR) and aldo-keto substrates have been used; such an observation supports the model structure choice.

iv) the high value of K_{eq} indicates a quick electron transfer in the (EAS) complex leading to fructose formation. It is also confirmed that the $NADP^+$ release from the (EA^+) complex represents the rate-limiting step, the estimated K_{AP} being smaller than the other equilibrium constants of the reaction chain. However, the estimated small equilibrium constant K_R of Table 2 reveal that the trig-

gering step (EA) + S ⇆ (EAS) is also a slow step in the chain.

v) another model confirmation is related to the fair reproduction of the experimental evidence of a very sharp initial decline in [NADPH] from the initial 6–35 mmol L^{-1} to low but quasi-constant levels of 0.1–0.3 mmol L^{-1}. In spite of this low [NADPH] level over the whole reaction domain (thousands of minutes), the kDG reduction does not stop but it occurs quantitatively due to the continuous decomposition of the (E^*A_y) inactive complex triggered by enzyme and co-enzyme consumption. In the absence of such a (co-)enzyme 'reservoir', a monotonous [NADPH] trajectory should be expected, similar to the exponential-like [kDG] decreasing curve.

vi) the experimental sharp decline of the initial [NADPH] over a few minutes is fully confirmed by the reported decline time (of a few seconds) measured by Grimshaw et al.[24] when reducing D-xylose using h-ALR. This evidence translates into an estimated high k_d constant, of the same order of magnitude as those reported for the h-ALR coupling to NADPH.[24] Even less favoured, the continuous slow transformation of the inactive E*A complex into an active (EA) complex (in our model via free enzyme and NADPH release) leads to the continuous availability of these species during the reaction, even if the quick NADPH consumption and ALR inactivation maintain their low level (see Figs. 1–4). The stoichiometric coefficient $y \approx 17.8$ milli-moles NADPH / U ALR (Table 2) indicates very high affinity of enzyme to NADPH, the inactive (E*A) complex lasting during the entire reduction process.

vii) the irreversible h-ALR enzyme inactivation occurs quite rapidly (ca. 10 min half-life according to the estimated k_i value) triggering the continuous release of active enzyme from its complex with the cofactor.

Several inhibition terms of the reduction rate have been neglected from the rate expression, according to the experimental observation of Leitner et al.,[14] i.e. the fructose low inhibition until 500 mmol L^{-1} concentration, and the negligible inhibition with the kDG substrate until 100 mmol L^{-1} levels (i.e. $[S][A] << K_R K_A$ in the rate r_P expression of Table 1). The continuous progress of the kDG reduction in spite of a low NADPH level confirms the Leitner et al.[14] conclusion that the reverse reaction can be neglected.

Conclusions

Derivation of an adequate and reliable kinetic model for a complex enzymatic process is a difficult task, requiring steady experimental efforts to obtain sufficient information on the process dynamics and its mechanism, and also extensive computational efforts to derive a comprehensible robust model with interpretable parameters. Such a model can be further valorised in developing engineering calculations, as long as simple separate observations cannot give the whole picture on the process characteristics, while its parameters do not vary with the reaction initial conditions.

In spite of slight overparameterization (i.e. 9 parameters vs. 4 observed variables recorded over 39 runs), leading to a lower estimability of two-three intercorrelated rate constants, the derived kinetic model for kDG reduction to fructose in the presence of ALR and NADPH presents fair adequacy, with parameter values comparable with those reported for similar systems. The confirmed 'core' mechanism employed in literature for describing various reactions catalyzed by ALR, h-ALR, and aldo-keto reductases, is also proved applicable to the studied system, being of satisfactory quality, robust, and with rate constants independent of the species initial concentrations but only on the reaction conditions.

The derived kinetic model reveals some interesting conclusions. The very high affinity of ALR for NADPH leads to the very fast and reversible formation of a complex ALR•NADPH of different forms (confirmed by literature data); only a small fraction of this complex is "active" for bonding the substrate, then leading to its reduction to fructose by an internal electron transfer in the ALR•NADPH•kDG complex. Several conformational re-arrangements of the enzymes occur during the successive Bi-Bi reaction steps, the slowest step confirmed being the $E'•A^+ \leftrightarrow E•A^+$ enzyme isomerization in order to release the $NADP^+$. Other inhibitory effects induced by the substrate or products are insignificant within the checked experimental range of [kDG] = 0–35 mmol L^{-1}, [NADPH] = 0–35 mmol L^{-1}, initial [ALR] = 0.0026–0.0060 U mL^{-1}.

The fast deactivation of the enzyme indicates a low level of active ALR during the reaction in spite of the slow decomposition of the quasi-stable (E^*A_y) complex. Consequently, the enzyme stabilization by immobilization appears to be crucial for further process development. On the other hand, the low level of active NADPH in the environment due to its very high affinity to the ALR, clearly indicates the requirement for a continuous *in-situ* regeneration of NADPH by using a parallel redox reaction.

The kinetic model parameters and predictions can be useful for further process development, while its structure can be translated easily to systems employing stabilized ALR forms. The model form can also be useful for conducting investigations into the possibility of immobilizing ALR on a

suitable support, or for predicting the process dynamics when performing *in-situ* regeneration of the cofactor by means of a suitable redox reaction, thus allowing further process optimization.

ACKNOWLEDGMENTS

The second author is grateful to the Biotehnos Co. (Otopeni, Romania) for the experimental facilities offered with generosity.

Symbols

c_j – species j concentration, mol L^{-1}
k_j – rate constants (in terms of mol L^{-1}, s, U L^{-1} units)
K_j – equilibrium constants, mol L^{-1}
m – number of observed species
N – total number of experimental points over all data sets (recording times)
p – number of model independent parameters
r_j – reaction rates (mol L^{-1} s^{-1}, U L^{-1} s^{-1})
s_y, s_y^2 – standard error deviation of the model, or its variance (in relative terms, Eq. 1)
t – time (s), or statistical Student test
y – stoichiometric coefficient, mol U^{-1}

Greeks

λ – eigenvalues of the inverse of the modified parameter covariance matrix[3]
σ – measurement error standard deviation, mol L^{-1}, U L^{-1}

Index

t – total

Superscipts

^ – estimated

Abbreviations

A – NADPH
A^+ – $NADP^+$
(h–)ALR – (human origin–) aldose reductases
E – aldose reductases
kDG – 2–keto–D–glucose
NAD(P)H – Nicotinamide adenine dinucleotide (phosphate) reduced form
P – fructose
S – substrate (kDG here)
TTC – 2,3,5–triphenyltetrazolium chloride
$\| \cdot \|_2$ – Euclidean norm

References

1. *Wang, P.,* Appl. Biochem. Biotechnol. **152** (2009) 343.
2. *Vasić-Rački, D., Findrik, Z., Presečki, A. V.,* Appl. Microbiol. Biotechnol. **91** (2011) 845.
3. *Maria, G.,* Chem. Biochem. Eng. Q. **18** (2004) 195.
4. *Gernaey, K. V., Lantz, A. E., Tufvesson, P., Woodley, J. M., Sin, G.,* Trends Biotechnol. **28** (2010) 346.
5. *Bhanuprakash Reddy, G., Satyanarayana, A., Balakrishna, N., Ayyagari, R., Padma, M., Viswanath, K., Mark Petrash, J.,* Mol. Vision **14** (2008) 593.
6. *Kaneko, M., Bucciarelli, L., Hwang, Y. C., Lee, L., Yan, S. F., Schmidt, A. M., Ramasamy, R.,* Ann. N. Y. Acad. Sci. **1043** (2005) 702.
7. *Yabe-Nishimura, C.,* Pharmacological Reviews **50** (1998) 21.
8. *Kubiseski, T. J., Hyndman, D. J., Morjana, N. A., Flynn, T. G.,* J. Biol. Chem. **267** (1992) 6510.
9. *Blakeley, M. P., Ruiz, F., Cachau, R., Hazemann, I., Meilleur, F., Mitschler, A., Ginell, S., Afonine, P., Ventura, O. N., Cousido-Siah, A., Haertlein, M., Joachimiak, A., Myles, D., Podjarny, A.,* Proc. Nati. Acad. Sci. U.S.A. **105** (2008) 1844.
10. *Akinterinwa1, O., Khankal, R., Cirino, P. C.,* Curr. Opin. Biotechnol. **19** (2008) 461.
11. *Kayser, M. M., Droleta, M., Stewart, J. D.,* Tetrahedron: Asymmetry **16** (2005) 4004.
12. *Monedero, V., Perez-Martinez, G., Yebra, M. J.,* Appl. Microbiol. Biotechnol. 86 (2010) 1003.
13. *Lindstad, R. I., Mc Kinley-Mc Kee, J. S.,* Eur. J. Biochem. **233** (1995) 891.
14. *Leitner, C., Neuhauser, W., Volc, J., Kulbe, K. D., Nidetzky, B., Haltrich, D.,* Biocatal. Biotransform. 16 (1998) 365.
15. *Srivastava, S. K., Ansari, N. H., Hair, G. A., Awasthi, S., Das, B.,* Metabolism **35** (1986) 114.
16. *Mayr, P., Petschacher, B., Nidetzky, B.,* J. Biochem. **133** (2003) 553.
17. *Grimshaw, C. E., Shahbaz, M., Putney, C. G.,* Biochemistry **29** (1990) 9947.
18. *Cromlish, J. A., Flynn, T. G.,* J. Biol. Chem. **258** (1983) 3416.
19. *Petrash, J. M.,* Cell. Mol. Life Sci. **61** (2004) 737.
20. *Neuhauser, W., Haltrich, D., Kulbe, K. D., Nidetzky, B.,* Biochem. J. **326** (1997) 683.
21. *Ryle, C. M. Tipton, K. F.,* Biochem. J. **227** (1985) 621.
22. *Chenault, H. K.., Whitesides, G. M.,* Appl. Biochem. Biotechnol. 14 (1987) 147.
23. *BRENDA* Enzyme database, TU Braunschweig (Germany), January 2013 release, http://www.brenda-enzymes.info/
24. *Grimshaw, C. E., Bohren, K. M., Lai, C. J., Gabbay, K. H.,* Biochemistry **34** (1995) 14356.
25. *Halder, A. B., Crabbe, M. J. C.,* Biochem. J. **219** (1984) 33.
26. *Shaked, Z., Wolfe, S.,* Methods Enzymol. **137** (1988) 599.
27. *Maria, G., Ene, M. D., Jipa, I.,* J. Mol. Catal. B: Enzym **74** (2012) 209.
28. *Ene, M. D., Maria, G.,* J. Mol. Catal. B: Enzym **81** (2012) 19.
29. *Slatner, M., Nagl, G., Haltrich, D., Kulbe, K. D., Nidetzky, B.,* Biocatal. Biotransform. **16** (1998) 351.
30. *Parmentier, S., Arnaut, F., Soetaert, W., Vandamme, E. J.,* Biocatal. Biotransform. **23** (2005) 1.
31. *Maria, G.,* Comput. Chem. Eng. **36** (2012) 325.

32. *Jiménez-Gonzáleza, C., Woodley, J. M.,* Comput. Chem. Eng. **34** (2010) 1009.
33. *Illanes, A.,* Enzyme biocatalysis, Springer Verlag, New York, 2008.
34. *Straathof, A. J. J., Adlercreutz, P.,* Applied biocatalysis, Harwood Academic Publ., Amsterdam, 2000.
35. *Liese, A., Hilterhaus, L.,* Chem. Soc. Rev. (2013), Advance Article (DOI**:** 10.1039/C3CS35511J)
36. *Rodrigues, R. C., Ortiz, C., Berenguer-Murcia, A., Torres, R., Fernández-Lafuente, R.,* Chem. Soc. Rev. (2013), Advance Article (DOI**:** 10.1039/C2CS35231A)
37. *Hernandez, K., Fernandez-Lafuente, R.,* Enzyme Microb. Technol. **48** (2011) 107.
38. *Fernandez-Lafuente, R.,* Enzyme Microb. Technol. **45** (2009) 405.
39. *Mateo, C., Palomo, J. M., Fernandez-Lorente, G., Guisan, J. M., Fernandez-Lafuente, R.,* Enzyme Microb. Technol. **40** (2007) 1451.
40. *Niroomandi, Z., Otadi, M., Panahi, H. A., Goharrokhi, M.,* International Proceedings of Chemical, Biological, and Environmental Engineering (IPCBEE) **25** (2011) 100.
41. *Iyer, P. V., Ananthanarayan, L.,* Process Biochem. **43** (2008) 1019.
42. *Leonida, M. D.,* Curr. Med. Chem. **8** (2001) 345.
43. *Slatner, M., Nagl, G., Haltrich, D., Kulbe, K. D., Nidetzky, B.,* Ann. N. Y. Acad. Sci. **20** (2002) 450.
44. *Liu, W., Wang, P.,* Biotechnol. Adv. **25** (2007) 369.
45. *Berenguer-Murcia, A., Fernandez-Lafuente, R.,* Curr. Org. Chem. **14** (2010) 1000.
46. *Dochain, D.,* J. Process Control **13** (2003) 801.
47. *Peacock, D., Boulter, A. D.,* Biochem. J. **120** (1970) 763.
48. *Lindstad, R. I., Mc Kinley-Mc Kee, J. S.,* FEBS Letters **408** (1997) 57.
49. *Ashwell, G.,* In: Methods in Enzymol 3, (Eds. Colowick, S. J., Kaplan, N.O.), pp. 75. Academic Press, New York, 1957.
50. *Segel, I. H.,* Enzyme kinetics, Wiley, New York, 1993.
51. *Treitz, G., Maria, G., Giffhorn, F., Heinzle, E.,* J. Biotechnol. **85** (2001) 271.
52. *Hayman, S., Kinoshita, J. H.,* J. Biol. Chem. **240** (1965) 877.
53. *Maria, G., Rippin, D. W. T.,* Chem. Eng. Sci. **48** (1993) 3855.
54. *Maria, G.,* In: Proceedings of the 22nd IASTED International Conference on Modelling, Identification, and Control, February 10–13, 2003, Innsbruck, Austria. IASTED/ ACTA Press, Anaheim (CA), 2003.